# Disturbance Rejection Using Self-Tuning ARMARKOV Adaptive Control with Simultaneous Identification

Harshad S. Sane, Ravinder Venugopal, and Dennis S. Bernstein

***Abstract*—In this paper we present a numerical and experimental investigation of the properties of the ARMARKOV adaptive control (AAC) algorithm with simultaneous identification. This algorithm requires a model of only the secondary path (control input to performance variable) transfer function which is identified online using the time-domain ARMARKOV/Toeplitz identification technique. For a 5-mode acoustic duct model, we present numerical as well as experimental results for single-tone, dual-tone, and broadband disturbance rejection. In the simulations and experiments we assume no knowledge of the disturbance signal.**

***Index Terms*—Acoustic duct, active noise control, adaptive control, ARMARKOV, discrete-time, disturbance rejection, identification.**

## I. Introduction

UNCERTAINTY in plant and disturbance modeling often renders fixed-gain control design based on off-line identification impractical. Consequently, adaptive controllers have been developed for active noise control [2], [5], [7]. In this paper we consider the ARMARKOV adaptive control (AAC) algorithm developed in [11]. The underlying model structure of AAC is the ARMARKOV model, which is a structurally constrained ARMA model with explicit impulse response (Markov) parameters [10]. The experimental results reported in [6], [8], [9], and [11] demonstrate the ability of the algorithm to suppress single-tone, dual-tone, and broadband disturbances with minimal plant and disturbance modeling. To do this, AAC requires a model of only the secondary path transfer function from the control input to the error variables. In particular, AAC does not require a model of the control-to-measurements transfer function nor does it require a model of the transfer function from plant disturbances to sensors and, unlike adaptive feedforward algorithms, it does not require measurements of the disturbance signals.

For experimental implementation the secondary path model is obtained by means of off-line identification using the ARMARKOV/Toeplitz recursive identification method of [1]. This identification algorithm yields transfer function models in ARMARKOV/Toeplitz form as required by the AAC algorithm. Least-squares identification based on ARMARKOV models is considered in [10].

The purpose of the present paper is to extend the AAC algorithm to further reduce the reliance on prior plant modeling. Specifically, we develop an indirect adaptive control extension of the AAC algorithm that includes simultaneous identification of the secondary path transfer matrix represented by the Toeplitz matrix $B_{zu}$. To do this we update the secondary path matrix $B_{zu}$ *at each time step* by means of the ARMARKOV/Toeplitz recursive identification method of [1].

To perform simultaneous identification in the presence of ambient disturbances, it is necessary to inject into the system through the control actuator an additional uncorrelated identification signal $u_{\rm ID}$. To oversee the proper functioning of simultaneous control and identification, a supervisory controller is used to make mode-switching decisions. These decisions include "switching controller adaptation," "toggling control signal ON/OFF," "resetting controller parameters to zero" and "switching simultaneous identification." The identification signal $u_{\rm ID}$ is turned OFF when identification is not being performed. The supervisory controller, which is a set of binary (ON/OFF) decision rules, makes its decisions by comparing present and past performance. The supervisory controller's decisions are thus based entirely on measured data so that no prior modeling is required.

## II. Standard Problem Representation

Consider the linear discrete-time system given by

$$z(k) = G_{zw}w(k) + G_{zu}u(k) \tag{1}$$

$$y(k) = G_{yw}w(k) + G_{yu}u(k) \tag{2}$$

where *disturbance* $w(k)$, the *control* $u(k)$, the *measurement* $y(k)$ and the *performance* $z(k)$ are in $\mathcal{R}^{m_w}, \mathcal{R}^{m_u}, \mathcal{R}^{l_y}$, and $\mathcal{R}^{l_z}$, respectively. The system transfer matrices $G_{zw}$ (primary path), $G_{zu}$ (secondary path), $G_{yw}$ (reference path), and $G_{yu}$ (control path) are in $\mathcal{R}^{l_z\times m_w}, \mathcal{R}^{l_z\times m_u}, \mathcal{R}^{l_y\times m_w}$, and $\mathcal{R}^{l_y\times m_u}$, respectively. The objective of the standard problem is to determine a controller $G_c \in \mathcal{R}^{m_u\times l_y}$ that produces a control signal $u(k) = G_c y(k)$ such that a performance measure involving $z(k)$ is minimized. A measurement of $z(k)$ is used to adapt $G_c$.

Next, the ARMARKOV/Toeplitz model of (1)–(2) [11] has the form

$$Z(k) = W_{zw}\Phi_{zw}(k) + B_{zu}U(k) \tag{3}$$

$$Y(k) = W_{yw}\Phi_{yw}(k) + B_{yu}U(k) \tag{4}$$

where $W_{zw}, W_{yw}, B_{zu}$ and $B_{yu}$ are block-Toeplitz matrices defined in [11]. The *extended performance vector* $Z(k)$, the *extended measurement vector* $Y(k)$ and the *extended control vector* $U(k)$ are defined by

$$Z(k) \triangleq [z(k) \quad \cdots \quad z(k-p+1)]^T$$

$$Y(k) \triangleq [y(k) \quad \cdots \quad y(k-p+1)]^T$$

$$U(k) \triangleq [u(k) \quad \cdots \quad u(k-p_c+1)]^T$$

Manuscript received June 15, 2000; revised October 4, 2000. Recommended by Guest Editors S. O. R. Moheimani and G. C. Goodwin.

H. S. Sane and D. S. Bernstein are with the Aerospace Engineering Department, University of Michigan, Ann Arbor, MI 48109 USA (e-mail: harshad@umich.edu; dsbaero@umich.edu).

R. Venugopal is with dSpace Inc., Northville, MI 48167 USA (e-mail: rvenugopal@dspaceinc.com).

Publisher Item Identifier S 1063-6536(01)00416-X.

where $p_c \triangleq \mu + n + p - 1$, $p$ is a positive integer, and the *ARMARKOV regressor vectors* $\Phi_{zw}(k)$ and $\Phi_{yw}(k)$ are shown in the first set of equations at the bottom of the page.

## III. ARMARKOV Adaptive Disturbance Rejection Algorithm

We use a strictly proper controller in ARMARKOV form of order $n_c$ with $\mu_c$ Markov parameters so that the control $u(k)$ is given by

$$\begin{aligned} u(k) = &\sum_{j=1}^{n_c} -\alpha_{c,j}(k)u(k-\mu_c-j+1) \\ &+ \sum_{j=1}^{\mu_c-1} H_{c,j-1}(k)y(k-j+1) \\ &+ \sum_{j=1}^{n_c} \mathcal{B}_{c,j}(k)y(k-\mu_c-j+1) \end{aligned} \tag{5}$$

where $H_{c,j} \in \mathcal{R}^{m_u \times l_y}$ are the Markov parameters of the controller. Next, define the *controller parameter block vector* as shown in (6) at the bottom of the page. Now from (5) it follows that $U(k)$ is given by

$$U(k) = \sum_{i=1}^{p_c} L_i \theta(k-i+1) R_i \Phi_{uy}(k) \tag{7}$$

where $\Phi_{uy}(k)$, $L_i$, and $R_i$ shown at the bottom of the page, with $q_1 \triangleq n_c m_u$ and $q_2 \triangleq (n_c + \mu_c - 1)l_y$. Thus, from (3) and (7) we obtain

$$\begin{aligned} Z(k) = &W_{zw}\Phi_{zw}(k) + B_{zu}\sum_{i=1}^{p_c} L_i\theta(k-i+1) \\ &\times R_i\Phi_{uy}(k). \end{aligned} \tag{8}$$

To evaluate the performance of the current value of $\theta(k)$ based on the behavior of the system during the previous $p_c$ steps, we define the *estimated performance* $\hat{Z}(k)$ by

$$\hat{Z}(k) \triangleq W_{zw}\Phi_{zw}(k) + B_{zu}\sum_{i=1}^{p_c} L_i\theta(k)R_i\Phi_{uy}(k) \tag{9}$$

which has the same form as (8) but with $\theta(k-i+1)$ replaced by the current parameter block vector $\theta(k)$. Using (9), we define the *estimated performance cost function*

$$J(k) = \frac{1}{2}\hat{Z}^T(k)\hat{Z}(k). \tag{10}$$

The gradient of $J(k)$ with respect to $\theta(k)$ is given by

$$\frac{\partial J(k)}{\partial \theta(k)} = \sum_{i=1}^{p_c} L_i^T B_{zu}^T \hat{Z}(k)\Phi_{uy}^T(k)R_i^T. \tag{11}$$

To evaluate $\hat{Z}(k)$, it follows from (3) and (9) that

$$\hat{Z}(k) = Z(k) - B_{zu}\left(U(k) - \sum_{i=1}^{p_c} L_i\theta(k)R_i\Phi_{uy}(k)\right). \tag{12}$$

The gradient (11) is used in the update law

$$\theta(k+1) = \theta(k) - \eta(k)\frac{\partial J(k)}{\partial \theta(k)} \tag{13}$$

where $\eta(k)$ is the *adaptive step size* given by

$$\eta(k) = \frac{1}{p_c\|B_{zu}\|_F^2\|\Phi_{uy}(k)\|_2^2}. \tag{14}$$

It is shown in [11] that the update law (13) with the step size (14) brings $\theta(k)$ closer to the minimizer of $J(k)$ with each time step. To implement the algorithm (11), (13), (14), we need only know the secondary path matrix $B_{zu}$.

---

$$\begin{aligned} \Phi_{zw}(k) &\triangleq [z(k-\mu) \quad \cdots \quad z(k-\mu-p-n+2) \quad w(k) \quad \cdots \quad w(k-\mu-p-n+2)]^T \\ \Phi_{yw}(k) &\triangleq [y(k-\mu) \quad \cdots \quad y(k-\mu-p-n+2) \quad w(k) \quad \cdots \quad w(k-\mu-p-n+2)]^T \end{aligned}$$

---

$$\theta(k) \triangleq [-\alpha_{c,1}(k)I_{m_u} \quad \cdots \quad -\alpha_{c,n_c}(k)I_{m_u} \quad H_{c,0}(k) \quad \cdots \quad H_{c,\mu_c-2}(k) \quad \mathcal{B}_{c,1}(k) \quad \cdots \quad \mathcal{B}_{c,n_c}(k)] \tag{6}$$

---

$$\begin{aligned} \Phi_{uy}(k) &\triangleq [u(k-\mu_c) \quad \cdots \quad u(k-\mu_c-n_c-p_c+2) \quad y(k-1) \quad \cdots \quad y(k-\mu_c-n_c-p_c+2)]^T \\ L_i &\triangleq \begin{bmatrix} 0_{(i-1)m_u \times m_u} \\ I_{m_u} \\ 0_{(p_c-i)m_u \times m_u} \end{bmatrix} \\ R_i &\triangleq \begin{bmatrix} 0_{q_1\times(i-1)m_u} & I_{q_1\times q_1} & 0_{q_1\times(p_c-i)m_u} & 0_{q_1\times(i-1)l_y} & 0_{q_1\times q_2} & 0_{q_1\times(p_c-i)l_y} \\ 0_{q_2\times(i-1)m_u} & 0_{q_2\times q_1} & 0_{q_2\times(p_c-i)m_u} & 0_{q_1\times(i-1)l_y} & I_{q_2\times q_2} & 0_{q_2\times(p_c-i)l_y} \end{bmatrix} \end{aligned}$$

## IV. AAC WITH SIMULTANEOUS IDENTIFICATION

In this section we discuss the self-tuning ARMARKOV/ Toeplitz controller along with simultaneous identification. The secondary path matrix $B_{zu}$ is obtained on-line using the time-domain identification technique discussed in [1]. In order to identify $B_{zu}$ in the presence of the disturbance $w(k)$, an uncorrelated signal $u_{\rm ID}$ is added to the control signal. An estimate $\hat{B}_{zu}(k)$ of $B_{zu}$ is obtained at every time instant $k$ and passed on to the AAC algorithm for the gradient update. For implementation, $B_{zu}$ in (11)–(13) is replaced by the current estimate $\hat{B}_{zu}(k)$.

A supervisory controller oversees the operation of simultaneous identification and control by making higher level decisions including toggling the control signal $u$, switching the controller adaptation, resetting the controller parameter vector $\theta(k)$ to zero and toggling the identification process (see Fig. 1). The additional signal $u_{\rm ID}$ is turned OFF when the identification process is OFF. The decisions of the supervisory controller are based on a measure of performance involving the RMS value of a $z$. Let $\mathcal{Z}_w$ be $w$th data-window of a fixed length $\Delta$ defined by $\mathcal{Z}_w \triangleq [z_{w\Delta+1} \ \cdots \ z_{(w+1)\Delta}]^T$. The supervisor has binary states `Z-grows`, `Z-reduces`, `Z-low` which are updated at the end of the current data window by comparing the values of $||\mathcal{Z}_w||$ and $||\mathcal{Z}_{w-1}||$. A well-defined set of rules shown in Table I is used to update the control variables `Cont` (control switch), `Adap` (adaptation switch), `Cont-reset` (resetting $\theta(k)$ to zero), `ID` (toggle identification) to their respective ON/OFF values depending on the states and previous values of control variables.

## V. NUMERICAL SIMULATIONS

The numerical simulations are based upon an acoustic duct model derived using modal decomposition of the acoustic pressure response of the duct to external acoustic inputs [3]. The modal model of the duct (length 6 ft) is restricted to five modes (tenth order). The model has two inputs, namely, a disturbance speaker situated at $x = 0.2$ and a control speaker situated at $x = 5.8$, $x$ being the coordinate along the length of the duct. The microphone sensors $y$ and $z$ are situated at $x = 0.3$ and $x = 5.9$, respectively. A schematic diagram of the acoustic duct is shown in Fig. 2.

The nominal tenth-order plant has its highest modal frequency at 378 Hz. The parameters chosen for simulation are $n = 10$, $\mu = 25$ and $p = 5$. The sampling time chosen is $t_s = 5 \times 10^{-4}$ sec. The AAC algorithm and the time-domain identification method are programmed in C in the form of a SIMULINK S-function block for use with MATLAB. The supervisory controller is written in C as a SIMULINK S-function in the form of a set of if-then-else statements which decide the ON/OFF values of the binary states `Z-grows`, `Z-reduces`, `Z-low` and control variables `Cont`, `Adap`, `Cont-reset`, `ID`. The simulations are performed for three different kinds of disturbances, namely, single tone (sinusoidal), dual-tone, and broadband. The controller parameters chosen for adaptation are $n_c = 10$, and $\mu_c = 25$. For all simulations $\theta(k)$, $\hat{B}_{zu}(k)$, $\hat{W}_{zu}(k)$ are initialized to zero. Initial conditions for the acoustic duct are assumed to be zero.

In the case of a single-tone disturbance at 320 Hz (see Fig. 3), the controller magnitude and phase plots (Fig. 4) show that the controller adapts to an internal model controller by placing high gain at the disturbance frequency. The plot also shows when the control variables `Cont`, `Adap`, `ID` are ON. The horizontal bars (Fig. 3) indicate the time intervals within which the respective variables are ON.

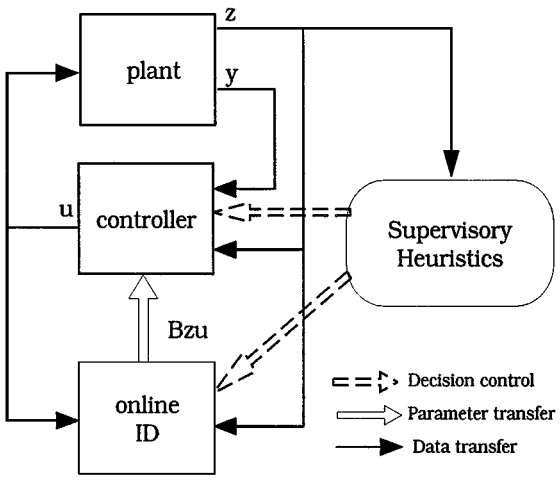


Fig. 1. Schematic of the operation of simultaneous identification and control with the supervisory controller.

For a dual-tone disturbance we choose nonharmonic frequencies 235 Hz and 320 Hz (see Figs. 5 and 6). As in the single-tone case, the controller adapts to an internal model to reject both tones. In the case of white noise (Fig. 7), the controller utilizes high gain in the bandwidth region and achieves up to 10–dB rejection of broad-band disturbance.

Next we examine a single-tone disturbance where we change the frequency of the disturbance (unknown to the algorithm) during operation. Specifically the disturbance frequency is changed from 350 Hz to 235 Hz at $t \approx 5.6$ s. Fig. 8 shows that after a small period of adaptation the new disturbance is successfully rejected. However it was noted that the algorithm converges such that the original peak (high gain at 350 Hz) is kept unchanged. Note that the supervisory controller turns OFF the adaptation (Fig. 8) when the controller converges and completely rejects the disturbance. However after the frequency change, adaptation is resumed to reject the new disturbance.

Finally, we test the ability of the controller to recover stability in the presence of a destabilizing uncertainty. To induce instability we change the sign of the control transfer matrix $G_{yu}$ during the simulation. A single-tone disturbance acts on the system throughout the simulation. Moreover, we restrict the allowable control level by saturating the control input so that $|u| \leq u_{\max}$. After the instability is introduced, the supervisory controller resumes controller adaptation. The algorithm manages to converge to a stabilizing controller and rejects the disturbance (Fig. 9). Large transients in the $z$ response are observed immediately after changing the sign of the control transfer matrix $G_{yu}$ ($t \approx 4.75$ s).

## VI. EXPERIMENTAL RESULTS

This section presents the results of an experimental study conducted on a one-dimensional acoustic duct. The duct of length 4.5 ft has a disturbance speaker and a control speaker attached

TABLE I
DECISION RULES FOR SIMULTANEOUS IDENTIFICATION AND CONTROL WITH THE SUPERVISORY CONTROLLER. HERE $\epsilon_1$ AND $\epsilon_2$ ARE SUPERVISOR DESIGN PARAMETERS

| Z-grows | | | | |
|---|---|---|---|---|
| IF $\|\mathcal{Z}_w\| > (1+\epsilon_1)\|\mathcal{Z}_{w-1}\|$ | Action Taken | | | |
| and IF $\downarrow$ THEN $\rightarrow$ | Cont | Adap | ID | Reset $\theta$? |
| Control ON | Step 1. ON | ON | OFF $\rightarrow$ ON | YES |
| Adaptation ON | Step 2. OFF | OFF | ON $\rightarrow$ ON | YES |
| Control ON, Adaptation OFF | | ON | OFF | NO |
| Control OFF, Adaptation ON | ON | | OFF | NO |
| Control OFF, Adaptation OFF | ON | ON | OFF | NO |

| Z-reduces | | | | |
|---|---|---|---|---|
| IF $\|\mathcal{Z}_w\| < \|\mathcal{Z}_{w-1}\|$ | Action Taken | | | |
| and IF $\downarrow$ THEN $\rightarrow$ | Cont | Adap | ID | Reset $\theta$? |
| Control ON, Adaptation ON | | | OFF | NO |
| Control ON, Adaptation OFF | | ON | OFF | NO |
| Control OFF, Adaptation ON | ON | | OFF | NO |
| Control OFF, Adaptation OFF | ON | ON | OFF | NO |

| Z-low | | | | |
|---|---|---|---|---|
| IF $\|\mathcal{Z}_w\| < \epsilon_2$ | Action Taken | | | |
| and IF $\downarrow$ THEN $\rightarrow$ | Cont | Adap | ID | Reset $\theta$? |
| Adaptation ON | | OFF | | NO |

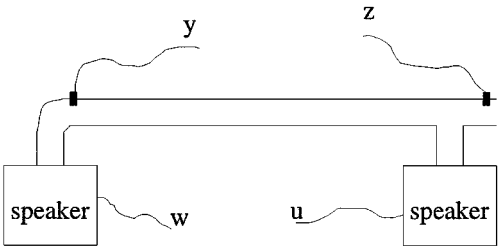


Fig. 2. Schematic of the acoustic duct system.

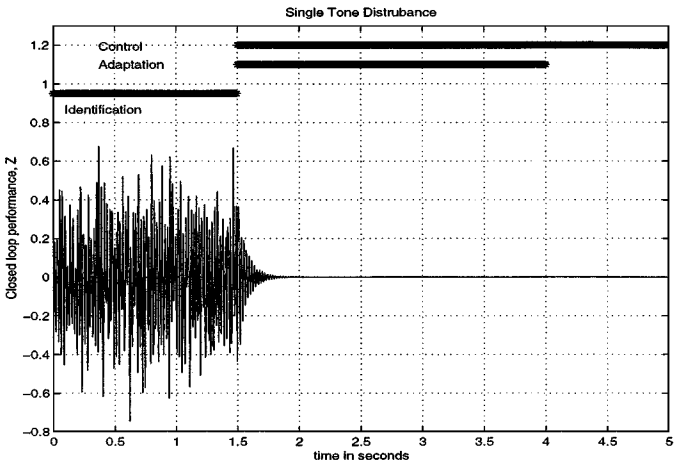


Fig. 3. Closed-loop response of the 5-mode acoustic duct to a sinusoidal disturbance at 320 Hz.

near opposite ends (see Fig. 2). Microphones measuring $y$ and $z$ are placed near the disturbance speaker and control speaker, respectively. The AAC algorithm, identification algorithm and the supervisory controller are programmed in C in the form of MATLAB S-functions and implemented on a dSPACE system with two 500 MHz real-time Alpha procesors. One Alpha processor is used to implement the AAC algorithm, while the other Alpha processor is used to implement the identification algorithm and supervisory controller. The architecture of the system allows data transfer between the processors as well as transfer from and to the acoustic duct system at each time step. Hence, at each time step $k$, an estimate $\hat{B}_{zu}(k)$ of the matrix $B_{zu}$ is transferred to the controller for gradient update. The sampling rate is chosen to be 1000 Hz. We use an SRS signal generator to generate the disturbance $w$.

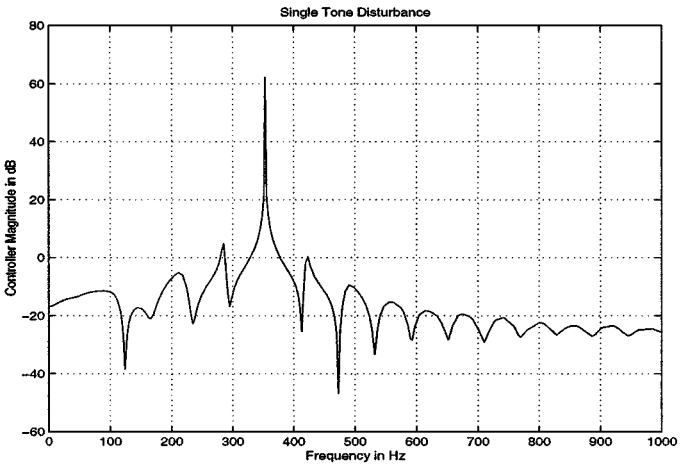


Fig. 4. Frequency response magnitude of the adapted controller for a sinusoidal disturbance at 350 Hz.

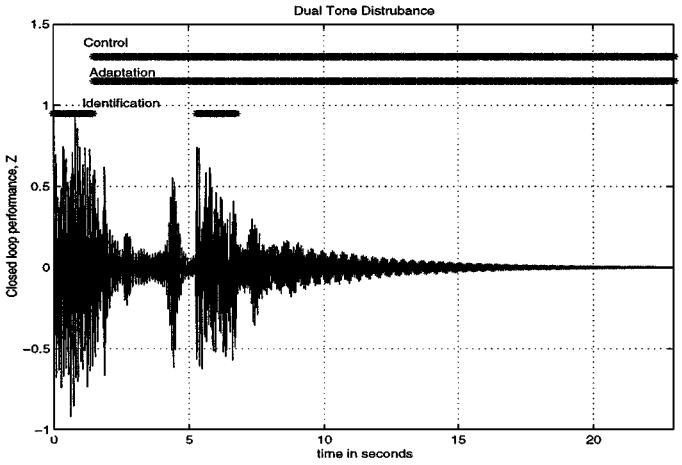


Fig. 5. Open-loop and closed-loop response of the 5-mode acoustic duct to a dual-tone disturbance (235 Hz, 320 Hz).

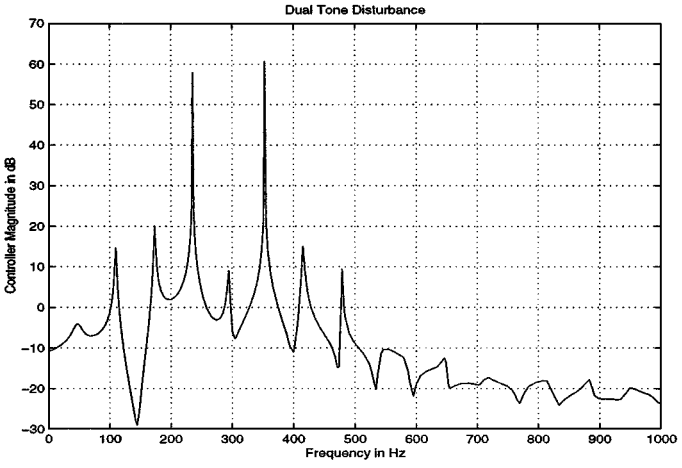


Fig. 6. Frequency response magnitude of the adapted controller for a dual-tone disturbance (235 Hz, 320 Hz).

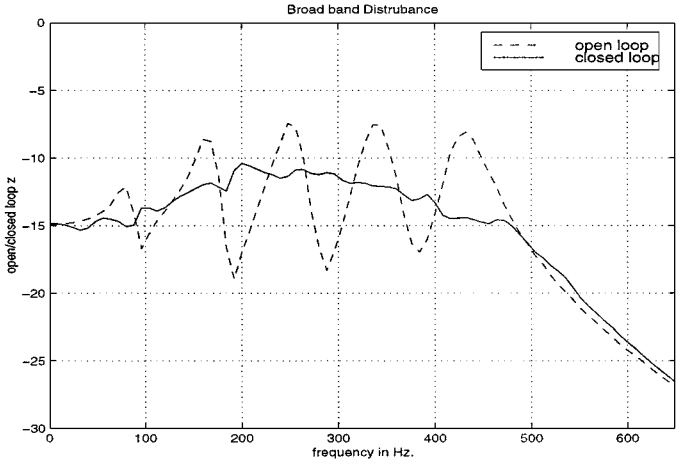


Fig. 7. Open-loop ($G_{zw}$) and closed loop ($\bar{G}_{zw}$) magnitude plots for a broadband disturbance.

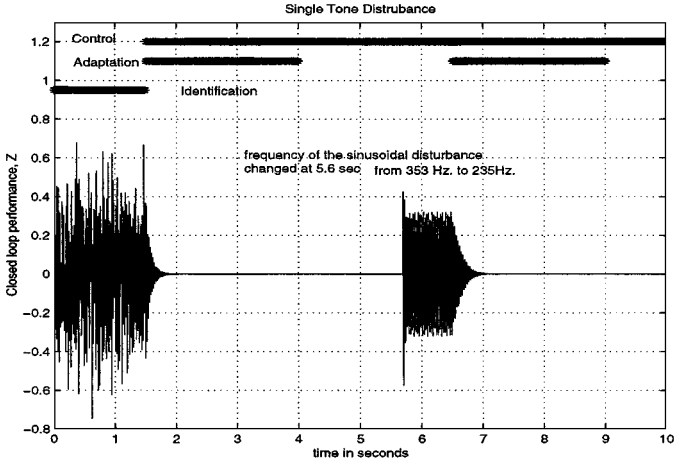


Fig. 8. In this simulation we change the frequency of a single-tone disturbance at an arbitrarily chosen time to demonstrate the ability of the controller to adapt to a change in the disturbance spectrum.

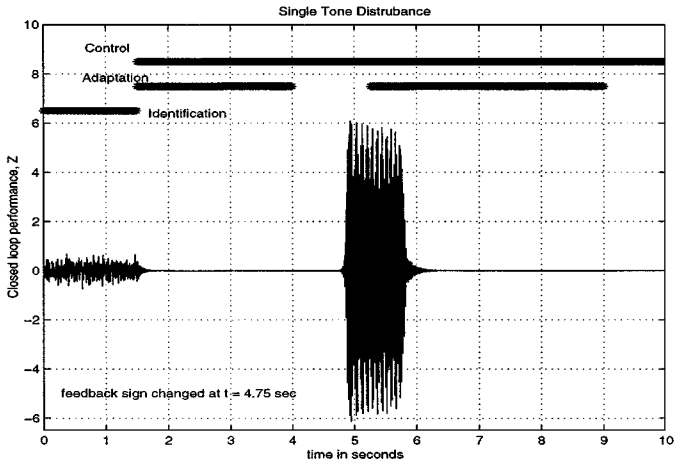


Fig. 9. In this simulation we destabilize the system by changing the sign of $G_{yu}$ at an arbitrarily chosen time ($t = 4.75$ sec) and allow the controller to adapt so as to restabilize the closed-loop system and reject the external disturbance.

Firstly, we consider single-tone disturbance rejection. A sinusoidal disturbance of frequency 190 Hz is injected into the system using the disturbance speaker. Next we change the frequency of the disturbance using the HP signal generator from 190 Hz to 250 Hz. After the change in frequency at $t = 10.5$ seconds, the supervisory controller performs identification for a

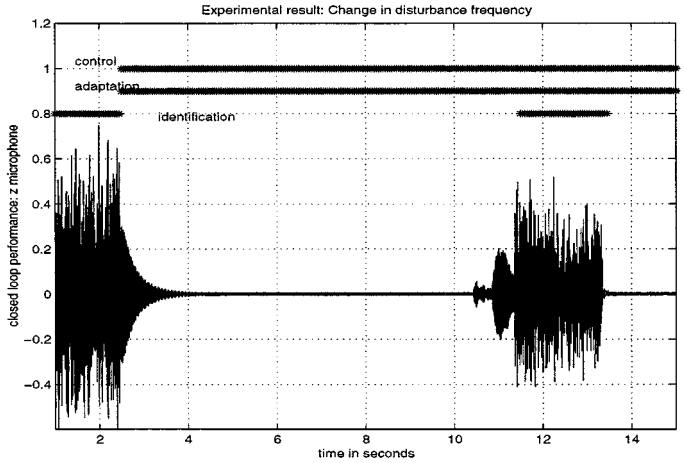


Fig. 10. Experimental result: In this experiment we change the frequency (190 Hz to 250 Hz) of the single-tone disturbance at an arbitrarily chosen time to demonstrate the ability of the controller to adapt to change in the disturbance spectrum.

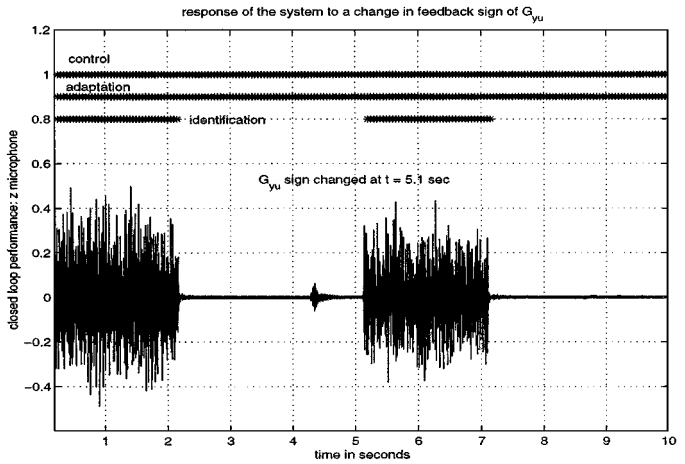


Fig. 11. Experimental result: In this experiment we change the feedback sign of the loop transfer function $G_{yu}$ at an arbitrarily chosen time ($t = 5.1$ s).

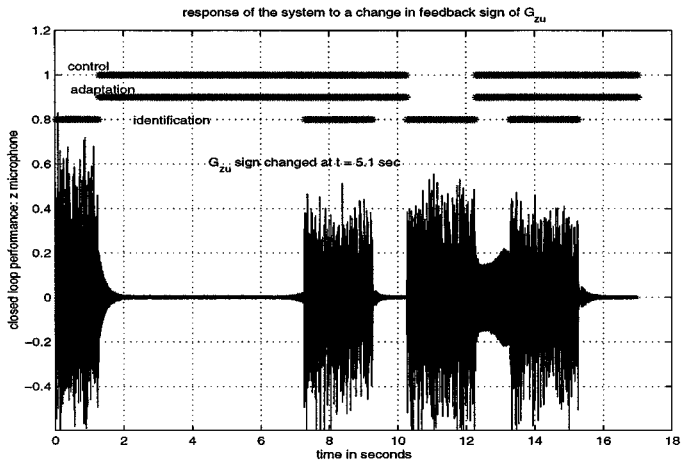


Fig. 12. Experimental result: In this experiment we change the feedback sign of the secondary path transfer function $G_{zu}$ at an arbitrarily chosen time ($t = 6.1$ s).

fixed time window. The controller then adapts to reject the new disturbance (see Fig. 10).

Next we investigate the performance of the combined control and identification algorithms under destabilizing conditions. To create these scenarios we change the sign of the control transfer function $G_{yu}$ and the secondary path transfer function $G_{zu}$. We do this by inverting the polarity of the microphone signals using the microphone preamplifiers. With $G_{yu}$ replaced with by $-G_{yu}$, the supervisor initiates identification of $B_{zu}$, which is unaffected. After a period of identification the instability in the system is overcome and the sinusoidal disturbance is rejected (see Fig. 11).

Next, with $G_{zu}$ replaced with by $-G_{zu}$, the sign of $B_{zu}$ is inverted and hence the supervisory controller needs to reidentify the plant several times to obtain a satisfactory estimate $\hat{B}_{zu}(k)$ of $B_{zu}$ (Fig. 12).

## VII. Conclusion

In this paper we performed computational and physical experiments involving the AAC algorithm with simultaneous identification. The performance of AAC was considered under a diverse set of conditions representing plant and disturbance uncertainty including perturbed disturbance spectrum, control input saturation, and control feedback and secondary path sign inversion. A supervisory controller was constructed to implement higher level control decisions for simultaneous control and identification. Experimental implementation validated the numerical results. A dual Alpha processor dSPACE system was used to simultaneously implement the identification and control algorithms. The properties illustrated by the present study will be useful in theoretical investigations of such guarantees.

## References

[1] J. C. Akers and D. S. Bernstein, "Time-domain identification using ARMARKOV/Toeplitz models," in *Proc. Amer. Contr. Conf.*, Albuquerque, NM, June 1997, pp. 191–195.

[2] R. L. Clark, W. R. Saunders, and G. P. Gibbs, *Adaptive Structures Dynamics and Control*. New York: Wiley, 1998.

[3] J. Hong, J. C. Akers, R. Venugopal, M.-N. Lee, A. G. Sparks, P. D. Washabaugh, and D. S. Bernstein, "Modeling, identification, and feedback control of noise in an acoustic duct," *IEEE Trans. Contr. Syst. Technol.*, vol. 4, pp. 283–291, 1996.

[4] J. Hong and D. S. Bernstein, "Bode integral constraints, colocation, and spillover in active noise and vibration control," *IEEE Trans. Contr. Syst. Technol.*, vol. 6, pp. 111–120, 1998.

[5] S. M. Kuo and D. R. Morgan, *Active Noise Control Systems*. New York: Wiley, 1996.

[6] S. L. Lacy, R. Venugopal, and D. S. Bernstein, "ARMARKOV adaptive control of self-excited oscillations of a ducted flame," in *Proc. Conf. Dec. Contr.*, Tampa, FL, Dec. 1998, pp. 4527–4528.

[7] P. A. Nelson and S. J. Elliott, *Active Control of Sound*. New York: Academic, 1993.

[8] H. Sane and D. S. Bernstein, "Active noise control using an acoustic servovalve," in *Proc. Amer. Contr. Conf.*, Philadelphia, PA, June 1998, pp. 2621–2625.

[9] T. Van Pelt, R. Venugopal, and D. S. Bernstein, "Experimental comparison of adaptive cancellation algorithms for active noise control," in *Proc. Conf. Contr. Appl.*, Hartford, CT, Oct. 1997, pp. 559–564.

[10] T. Van Pelt and D. S. Bernstein, "Least squares identification using $\mu$-Markov parameterizations," in *Proc. Conf. Decision Contr.*, Tampa, FL, Dec. 1998, pp. 618–619.

[11] R. Venugopal and D. S. Bernstein, "Adaptive disturbance rejection using ARMARKOV system representations," *IEEE Trans. Contr. Syst. Technol.*, vol. 8, pp. 257–269, 2000.